Analysis of CO2 Jet's Temperature by BOS Method for Applications in Cryogenic Machining

Koulekpa Koffi Samuel, Michael Deligeant, Hélène L. Elias-Birembaux, Frederic Rossi, Gerard Poulachon

MIC2023
23rd Machining Innovations Conference for Aerospace Industry

Proceedings are available on SSRN: www.ssrn.com

SSRN Proceedings Hosted on SSRN.com

MIC Procedia (2023) 093–098

23rd Machining Innovations Conference for Aerospace Industry 2023 (MIC 2023),
29th and 30th November 2023, Hannover, Germany

Analysis of CO_2 Jet's Temperature by BOS Method for Applications in Cryogenic Machining

Koffi Samuel Koulekpa [a,*], Michael Deligant[b], Hélène Elias-Birembaux[a], Frédéric Rossi[a], Gérard Poulachon[a]

[a]*Arts et Metiers Institute of Technology, LaBoMaP, Université Bourgogne Franche-Comté, HESAM Université, F-71250 Cluny, France*
[b]*Arts et Métiers Institute of Technology, CNAM, LIFSE, HESAM University, F-75013 Paris, France*

* Corresponding author. Tel.: : +3385595330; *E-mail address:* koffi.koulekpa@ensam.eu

Abstract

In order to face the challenges in machining difficult-to-cut materials as nickel and titanium alloys, many cooling methods have been developed through the years, among which is the usage of supercritical carbon dioxide ($scCO_2$). By combining the cooling provided by the expansion of the CO_2 jet, and the $scCO_2$ solvent properties (for dissolving lubricants), it is possible to reach higher tool life and productivity, with respect to the other classical cooling methods. The purpose of this study is to compare the Background Oriented Schlieren (BOS) method with thermocouple measurements in the context of CO_2 jets, whether in liquid or supercritical state. A typical BOS setup using an enlightened background pattern and a high-speed camera was used to determine the temperature of CO_2 jets. While the trend of BOS centerline temperature aligns with that of the thermocouple measurements, there exist noticeable disparities between them. These discrepancies average around 20°C in favourable instances and can reach up to 60°C in the most extreme cases. These findings underscore the need to continue the investigation to identify areas for improvement. This pursuit is essential to achieve accurate results for using this method in the development of future temperature models for CO_2 jets.

Keywords: Supercritical Carbon Dioxide; Background Oriented Schlieren method; Jet expansion; Cutting fluids; Tool life

1. Introduction – State of art

1.1. Assisted-machining

The control of cutting temperature when machining difficult-to-cut materials, such as titanium and nickel-based alloys, has a considerable impact on tool-life, wear mechanisms, surface integrity, production time, and chip flow [1]...This has been achieved through the years by using flood coolants, which provide the needed lubrication and cooling at the tool/part interface [2]. But the cost and health risks linked to their usage have led to the development of other techniques such as Minimum Quantity Lubrication (MQL), liquid Nitrogen (LN_2), liquid CO_2 and supercritical CO_2 ($scCO_2$) [3]. This latter has demonstrated a great interest due to its influence on the process.

1.2. Supercritical CO_2 in machining processes

When raised to the supercritical state (above 74 bars and 31°C), CO_2 can dissolve some particles of oils or lubricants given that $scCO_2$ is widely recognized as an environmentally friendly solvent [4]. The combination of this lubrication and

the cooling effect produced by the expansion (Joule-Thompson effect [5]), when delivered to the cutting zone, allows the decrease of the temperature produced in the process [6,7], leading to longer tool life and good surface integrity [8,9], often better than traditional MQL or flood coolants.

1.3. Cooling ability of CO_2 jets

In order to analyze the CO_2 jet properties, Mulyana et al. [6], studied the cooling rate for $scCO_2$ and $scCO_2$ + MQL jets, by placing a K-thermocouple in a heated carbide rod, for the pressure values of 78.8, 59.6 and 104 bars. A maximum cooling rate of 13.6°C/s was observed for $scCO_2$ + MQL at 104 bars.

Gross et al. [10] placed a thermocouple in different positions along the axis of a CO_2 jet and recorded the centreline profile temperature for nozzles of 0.2, 0.3 and 0.5 mm diameter. They noticed that increasing the diameter did not lower the minimum temperature but rather enlarged the cold zone.

Pursell et al. [11] placed a thermocouple rack in liquid and gaseous jets of CO_2, using 2 mm and 4 mm orifices. They recorded a decrease of temperature near the nozzle output (down to -80 °C), before the warming of the jet as the downstream distance increases. Khalil et al. [12] modelled the density contours after expansion of $scCO_2$ flows into air, and compared the results to shadowgraph measurements (wave structures) and impact pressures on a plate placed in front of the jet.

Few works studied the properties of the whole jet (density, phase and temperature). Accessing and establishing a whole jet temperature model could be useful for modelling CO_2 jets and their impacts on cutting processes. This latter temperature model could be paired to a heat transfer coefficient model, to properly simulate $scCO_2$-assisted machining operations. This preliminary work aims then to study the temperature during the expansion of the jet using Background Oriented Schlieren method (BOS). The results were compared to a distinct thermocouple rack measurement taken under identical conditions for validation purposes. This comparative analysis serves the larger purpose of facilitating the future development of a comprehensive jet temperature model.

2. Principles of the BOS method

The Background Oriented Schlieren method is a non-intrusive technique used to characterise the density and temperature gradients in inhomogeneous fluids [13–15]. It consists in recording with a camera, focused on a background pattern enlightened from behind (figure 1), two images corresponding to the scene without, and with the fluid. The displacement field obtained by cross-correlation algorithms is the image of the gradients contained within the fluid. This displacement field is used to calculate the refractive index field by different approaches:

- The Poisson equation in the case of 2D plane fluids, when the width of the medium is known [16],
- Abel Transform for axisymmetric fluids using the vertical displacement [17,18],
- Other tomographic reconstruction algorithms [19].

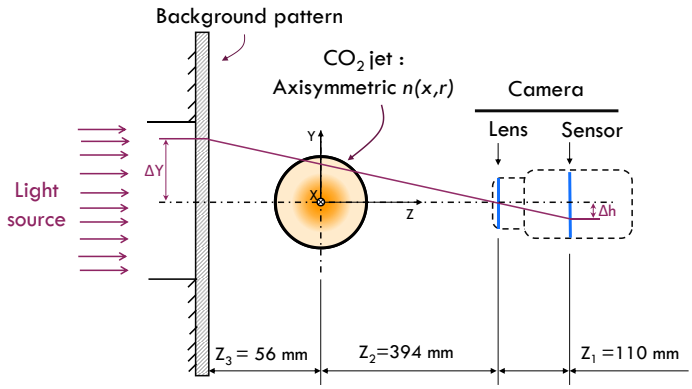

Fig. 1 Illustration of ray path in the BOS experiment

In this work, the axisymmetric theory is used, as the type of jets studied here are axisymmetric due the rounded jets nozzle used.

The notation described below refer to figure 1. The equations of the BOS are well established in the literature, so only the key steps are listed here. Using the principle of Fermat and the small refraction angles principles [20,21], the vertical deflection can be expressed as a function of the index of refraction [17,22] :

$$\varepsilon(y) = \int_{|y|}^{\infty} \frac{rdr}{\sqrt{r^2-y^2}} \left(\frac{y}{r} \frac{\partial n(x,r)}{\partial r} \right) = \frac{\Delta h(x,y)}{MZ_3} \qquad (1)$$

Where $\varepsilon(y)$ is the vertical angular deflection, $n(x,r)$ is the spatial axisymmetric distribution of the index of the refractive index with $r=\sqrt{y^2+z^2}$, y the vertical component on the jet plane, and Δh the vertical displacement recorded by the sensor of the camera. Δh is linked to the displacement ΔY on the background plane, by the distance Z_3 and the magnification factor M of the camera. The factor M is not taken into account in the following calculations because it is already included in the calibration of the camera during the experiments [17].

Using the inverse Abel transform, the index refraction field is extracted from equation 1 to equation 2:

$$n(r,x) = n_0 + \frac{1}{\pi Z_3} \int_r^{\infty} dr' r' \int_{r'}^{\infty} \frac{dh}{\sqrt{h^2-r'^2}} \frac{\partial}{\partial h} \left(\frac{\Delta h(x,h)}{h} \right) \qquad (2)$$

n_0 being the refractive index of the ambient air. Using the ideal gas law and the Gladstone-Dale [23] relation, in equation 3 (with ρ being the density, p the pressure, R the gas constant and T the temperature),

$$n = 1 + G\rho = 1 + G\frac{p}{RT} \qquad (3)$$

the density and temperature gradients can be calculated by equations 3 and 4 as:

$$n(r,x)-1=(n_0-1)\frac{\rho(r,x)}{\rho_0} \quad (4)$$

With ρ_0 the density of ambient air;

$$\frac{T(r,x)}{T_0}=\left[\left(\frac{n(r,x)}{n_0}-1\right)\left(\frac{RT_0}{GP_0}+1\right)+1\right]^{-1} \quad (5)$$

With $G = 2.26 \times 10^{-4}\, m^3/kg$ being the Gladstone-Dale coefficient of CO_2 [19], T_0 and P_0, the ambient temperature and pressure respectively.

3. Experimental setup

3.1. BOS setup

A *FlowSense Cx 5M-124* camera with a 2448x2048 pixel sensor was placed on a tripod and focused on a printed background pattern generated by the Dantec Dynamics software (DynamicStudio 8.1). This pattern was placed on a transparent plexiglas plate enlightened from behind by a simple lamp as shown on figure 2. The area of interest was set to 40x40 mm because, the tool-nozzle distance in machining operations is rarely over 40mm. This zone of interest was vertically centered in relation to the nozzle axis, aiming to achieve symmetry in the captured displacement images as much as possible.

Round jet sapphire nozzles with diameters of 0.1 mm and 0.25 mm, sourced from TESCHKE, were employed for these preliminary tests. The conditions should be limited in pressure and temperature to avoid an opaque jet (with ice) leading to poor displacements measurements. Three conditions are presented in Table 1, to investigate the feasibility of studying CO_2 jets temperature (liquid and supercritical) by the BOS method. In Table 1, D stands for diameter, P and T, for the upstream pressure and temperature, defining the CO_2 state before the nozzle (liquid or supercritical). Validating this method would subsequently contribute to the development of a jet temperature model *T = f(D, P, T)* with the aforementioned parameters serving as inputs.

The main distances on the experimental setup are illustrated on figure 1. The recorded displacements calculated in DynamicStudio, were postprocessed in Python using the pyAbel [24] library to perform the inverse Abel transform and calculate the temperature distribution.

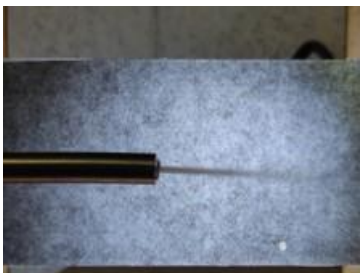

Fig. 3 BOS setup with enlightened pattern

Table 1: Conditions used in the experiments

D = 0.1 mm	P (bars)	60	100
	T (°C)	30	
D = 0.25 mm	P (bars)	80	
	T (°C)	40	

3.2. Thermocouple measurements

A thermocouple rack was designed to record the centerline-temperature in the CO_2 jets for liquid and supercritical conditions, as illustrated on figure 3. It consists in thirteen (13) K+ and K- thermocouple wires welded and fixed to springs, spaced by 5 mm, a part from the last two which are spaced by 15 mm. The springs attached to the frame allow the alignment of the welding points on the same line. The acquisition set Ni9205 +cDAQ-9171 is used to record the temperature during the experiments, with a 15kHz frequency.

A mean value is computed from the data collected by each individual thermocouple. In the case of non-stable jets, when the formation of dry ice occurs, the stable measured zone is used for calculations. The thermocouple measurements conditions, conducted under the same conditions are outlined in Table 1 will serve as a benchmark for evaluating the results obtained through the BOS method.

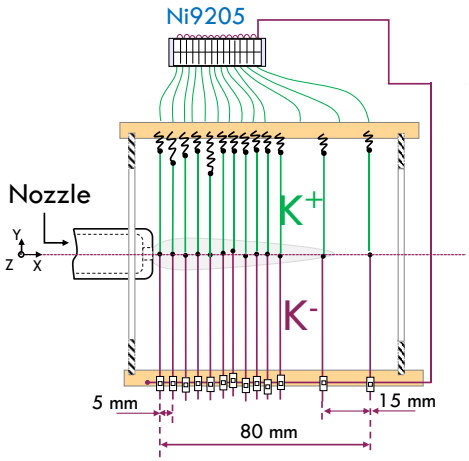

Fig. 2. Illustration of the thermocouple rack

3.3. $ScCO_2$ production device

The machine employed for the experiments, shown on figure 4, is a custom-built system designed for delivering liquid and supercritical CO_2 [25]. The mix of liquid and gaseous CO_2, taken from the CO_2 bottles is cooled down at 10°C to ensure it is in a liquid state before compression and heating, to reach the supercritical state. The $scCO_2$ is stocked in a pressure vessel before delivered throughout the nozzle. The pressure and temperature conditions can be provided to

Fig. 6 Liquid and supercritical CO_2 delivery machine

operate with either liquid or supercritical CO_2. These conditions are measured by pressure sensors and thermocouples placed before the nozzle, and regulated by a controller unit.

4. Results

The figures 5a and 5b illustrate respectively an example of the jet and vertical displacement recorded for the supercritical condition. The dashed rectangle zone illustrates an example of the analyzed zone. After applying the previously described BOS method to the axisymmetric displacement distribution, the resulting temperature maps are depicted in figure 6.

The radial distributions extracted at x = 10 mm and the centerline temperatures are plotted on figure 7 for each condition. The corresponding thermocouples measurements are added on figure 7b, c and d.

Similar to the findings of Gross et al. [10], the core jet dimension is larger for D = 0.25 mm (extending up to 15 mm in the axial direction on Figure 6c), while it is smaller for 6a and 6b, corresponding to a diameter of D = 0.1 mm. The decrease of the centerline temperature (figure 7c and 7d) recorded near the output of the nozzle before the warming with downstream distance, is similar to the behavior modeled by Pursell et al. [11], which correspond to the expansion zone. But for the condition D0.1P60T30 (figure 7b), the BOS temperature values in the expansion zone are unexpectedly far above the thermocouple's measurements (A 60°C gap at x=0). Knowing that changing the diameter should not lower that much the cold temperature values [10], there is a need of repetition to state about possible source of error.

The gap between the BOS measurement and the thermocouple measurement (realized in the same conditions) could be explained either by the bias of ideal gas law used in the BOS method which suppose a constant pressure in the jet core, or the fact that there could be slight changes in the jet from one experiment to another (BOS to thermocouple), even though the upstream conditions are the same. However, the strength of the BOS technique lies in its ability to capture both radial and axial density and temperature gradient distributions, thereby offering more comprehensive and valuable insights compared to discrete thermocouple measurements.

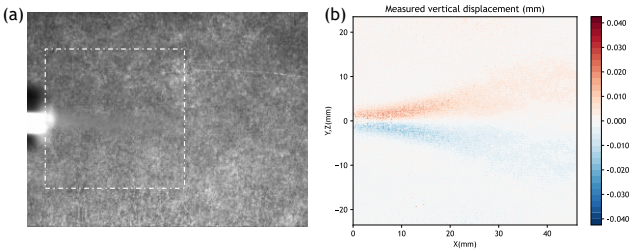

Fig. 5. a. Image of the jet recorded during experiment (b) Example of vertical displacement

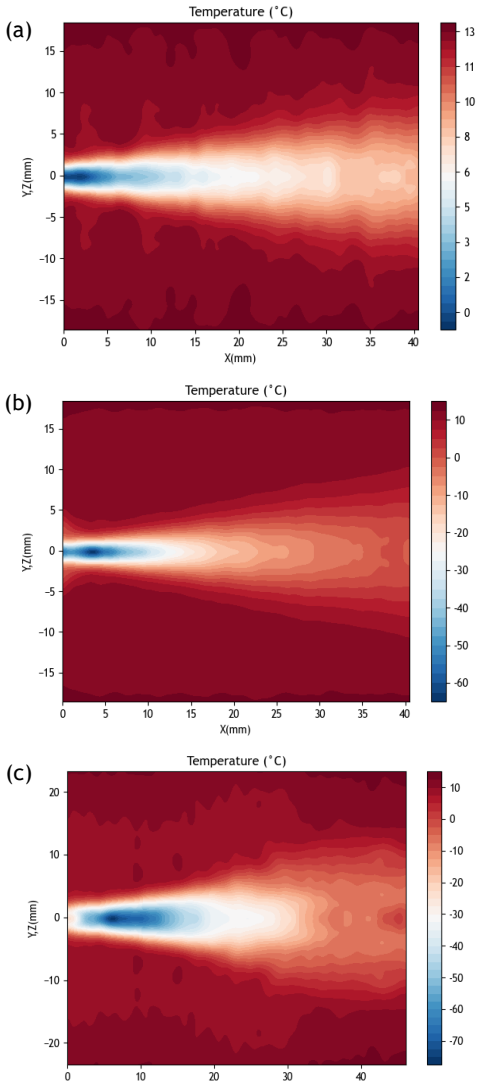

Fig. 4 Temperature maps obtained for conditions (a)D0.1P60T30 (b)D0.1P150T30 and (c)D0.25P80T40

A difficulty noticed in the application of the BOS method is the formation of dry-ice for higher supercritical condition or higher diameter values, which lead to poor results because of the jet's opacity. The conditions to be used in future applications of the BOS method on CO_2 jets, should be carefully considered to prevent such occurrences. For instance, with a nozzle diameter of 0.25 mm, pressures higher than 100 bars often leads to an opaque jet with ice.

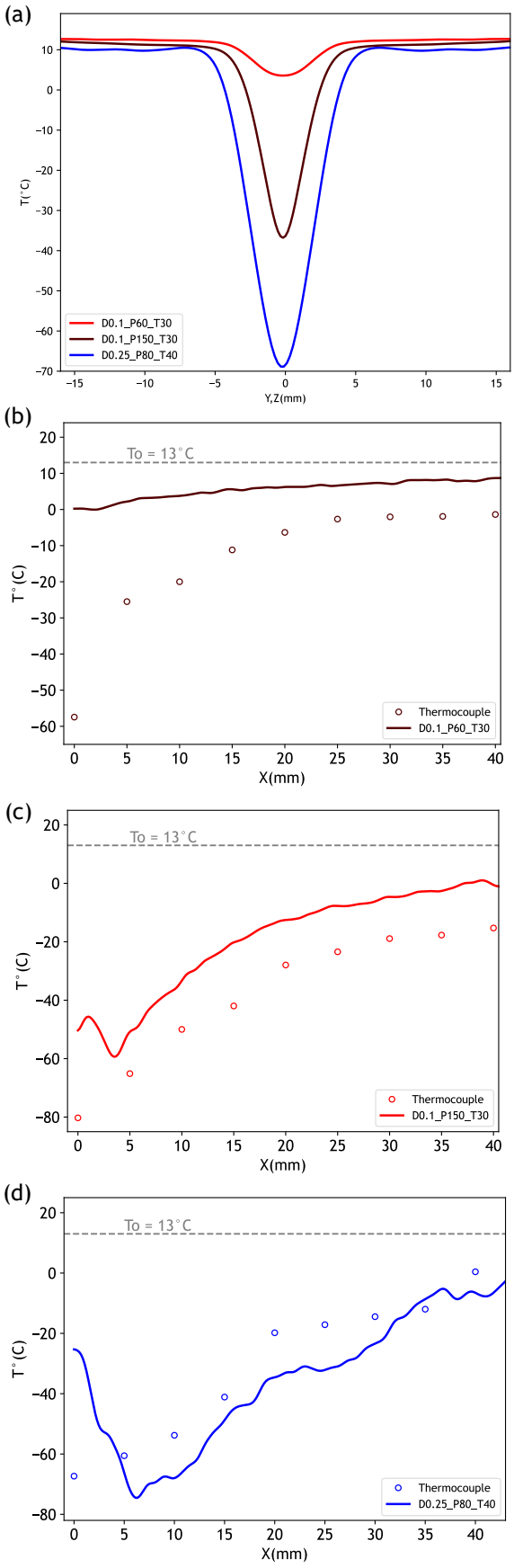

Fig. 7. a. Radial temperature distribution extracted at x = 10 mm BOS centreline temperatures against thermocouples measurements, for (b)D0.1P60T30 (c)D0.1P150T30 and (d) D0.25P80T40

Conclusion and perspectives

In the present work, the Background Oriented Schlieren method has been applied to liquid an supercritical CO_2 and benchmarked to thermocouple measurements. The expansion behavior described by Pursell et al. [11], was observed, resulting in a near-nozzle temperature decrease reaching as low as -80°C. Discrepancies were identified between the BOS results and those obtained through thermocouples:

- Regular error of about 20°C for condition D0.25P80T40 and D0.1P150T30, which could be reduced with careful and meticulous experiments execution,
- Unexpected gap of 60°C in the expansion zone for D0.1P60T30 which will need repetition to uncover the source of such gap.

Nevertheless, this method has shown potentialities to establish a model of temperature describing the spatial axisymmetric distribution of CO_2 jets, based on existing models [26]. Future works will focus on implementation of careful and repeated design of experiment to create a robust database for model development. This model will subsequently find application in simulations of liquid and supercritical CO_2-assisted cutting processes.

Acknowledgements

The authors would like to thank the funders of this research: INSTITUT CARNOT ARTS, CETIM and Bourgogne Franche-Comté council.

References

[1] F. Laforce, CETIM_Etude comparative du fraisage assisté par cryogénie - Version française et anglaise, *Cetim - Centre technique des industries mécaniques*. (2019). https://www.cetim.fr/mecatheque/Resultats-d-actions-collectives/Etude-comparative-du-fraisage-assiste-par-cryogenie-Version-francaise-et-anglaise (accessed November 5, 2021).

[2] K. Zheng Yang, A. Pramanik, A.K. Basak, Y. Dong, C. Prakash, S. Shankar, S. Dixit, K. Kumar, and N. Ivanovich Vatin, Application of coolants during tool-based machining – A review, *Ain Shams Engineering Journal*. (2022) 101830. doi:10.1016/j.asej.2022.101830.

[3] I.S. Jawahir, H. Attia, D. Biermann, J. Duflou, F. Klocke, D. Meyer, S.T. Newman, F. Pusavec, M. Putz, J. Rech, V. Schulze, and D. Umbrello, Cryogenic manufacturing processes, *CIRP Annals*. **65** (2016) 713–736. doi:10/gjnvsk.

[4] J.A. Hyatt, Liquid and supercritical carbon dioxide as organic solvents, *ACS Publications*. (2002). doi:10.1021/jo00200a016.

[5] L. Proud, N. Tapoglou, and T. Slatter, A Review of CO2 Coolants for Sustainable Machining, *Metals*. **12** (2022) 283. doi:10.3390/met12020283.

[6] T. Mulyana, The influence of cryogenic supercritical carbon dioxide cooling on tool wear during machining high thermal conductivity steel, *Journal of Cleaner Production*. (2017) 13. doi:10/gbw9wv.

[7] E.A. Rahim, A.A. Rahim, M.R. Ibrahim, and Z. Mohid, Experimental Investigation of Supercritical Carbon Dioxide (SCCO2) Performance as a Sustainable Cooling Technique, *Procedia CIRP*. **40** (2016) 637–641. doi:10.1016/j.procir.2016.01.147.

[8] N. Tapoglou, C. Taylor, and M. Christos, Milling of aerospace alloys using supercritical CO2 assisted machining, *Procedia CIRP*. **101** (2021) 370–373. doi:10/gmwp69.
[9] J. Khosravi, B. Azarhoushang, M. Barmouz, R. Bösinger, and A. Zahedi, High-speed milling of Ti6Al4V under a supercritical CO2 + MQL hybrid cooling system, *Journal of Manufacturing Processes*. **82** (2022) 1–14. doi:10.1016/j.jmapro.2022.07.061.
[10] D. Gross, M. Appis, and N. Hanenkamp, Investigation on the productivity of milling ti6al4v with cryogenic minimum quantity lubrication, *MM Science Journal*. (2019). doi:10/gmxf5t.
[11] M. Pursell, Experimental investigation of high pressure liquid CO2 release behaviour, (2012).
[12] I. Khalil, and D.R. Miller, The structure of supercritical fluid free-jet expansions, *AIChE Journal*. **50** (2004) 2697–2704. doi:10.1002/aic.10285.
[13] S.B. Dalziel, G.O. Hughes, and B.R. Sutherland, Whole-field density measurements by 'synthetic schlieren,' *Experiments in Fluids*. **28** (2000) 322–335. doi:10.1007/s003480050391.
[14] L. Venkatakrishnan, Density Measurements in an Axisymmetric Underexpanded Jet by Background-Oriented Schlieren Technique, *AIAA Journal*. **43** (2005) 1574–1579. doi:10.2514/1.12647.
[15] M. Raffel, Background-oriented schlieren (BOS) techniques, *Exp Fluids*. **56** (2015) 60. doi:10.1007/s00348-015-1927-5.
[16] O.S. Jensen, Optical density and velocity measurements in cryogenic gas flows, Swiss Federal Institute of Technology Zurich, 2003. https://doi.org/10.3929/ethz-a-004621600 (accessed February 13, 2023).
[17] D. Kaganovich, L.A. Johnson, A.A. Mamonau, and B. Hafizi, Benchmarking background oriented schlieren against interferometric measurement using open source tools, *Appl. Opt., AO*. **59** (2020) 9553–9557. doi:10.1364/AO.406301.
[18] T.A. Sipkens, S.J. Grauer, A.M. Steinberg, S.N. Rogak, and P. Kirchen, New transform to project axisymmetric deflection fields along arbitrary rays, *Meas. Sci. Technol.* **33** (2021) 035201. doi:10.1088/1361-6501/ac3f83.
[19] S. Grauer, A. Unterberger, A. Rittler, K. Daun, A. Kempf, and K. Mohri, Instantaneous 3D flame imaging by background-oriented schlieren tomography, *Combustion and Flame*. **196** (2018). doi:10.1016/j.combustflame.2018.06.022.
[20] Principles of Optics - M.Born, E. Wolf, Page 128-130, Pargamon Press Oxford 1959, (n.d.). https://cdn.preterhuman.net/texts/science_and_technology/physics/Optics/Principles%20of%20Optics%20-%20M.Born,%20E.%20Wolf.pdf (accessed March 7, 2023).
[21] T.E. Walsh, and K.D. Kihm, Tomographic reconstruction of laser speckle photography for axisymmetric flame temperature measurement, *Journal of Flow visualization and Image processing*. **2** (1995) 299–310. http://minsfet.utk.edu/publications/1995_Tomographic%20Deconvolution%20of%20Laser.pdf (accessed February 28, 2023).
[22] A. Moumen, D. Laboureur, J. Gallant, and P. Hendrick, A new approach for the reconstruction of axisymmetric refractive index fields from background-oriented schlieren measurements, *Shock Waves*. **32** (2022) 313–318. doi:10.1007/s00193-022-01071-9.
[23] Vasilev L.A., Schlieren methods, *Israel Program for Scientific Translations*, 1971.
[24] S. Gibson, D.D. Hickstein, R. Yurchak, M. Ryazanov, D. Das, and G. Shih, PyAbel/PyAbel: v0.9.0, (2022). doi:10.5281/zenodo.7438595.
[25] K.S. Koulekpa, H. Birembaux, F. Rossi, and G. Poulachon, Etude expérimentale de l'usinage du Ti6Al4V sous assistance CO2 supercritique, in: 2022. https://hal.science/hal-04011776 (accessed June 1, 2023).
[26] N.K. Joshi, S.N. Sahasrabudhe, K.P. Sreekumar, and N. Venkatramani, Variation of axial temperature in thermal plasma jets, *Meas. Sci. Technol.* **8** (1997) 1146. doi:10.1088/0957-0233/8/10/016.